Front. Phys. China, 2007, 2(4): 440−445
DOI 10.1007/s11467-007-0055-y

RESEARCH ARTICLE

**LÜ Xiao-jing, WU Ju, XU Bo, ZENG Yi-ping,
WANG Biao-qiang, WANG Zhan-guo**

InAs nanostructures on InP (001) substrate with the insertion of a superthin AlAs layer

Abstract An AlAs layer of two or three monolayers was inserted beneath the strained InAs layer in the fabrication of InAs nanostructure on the $In_{0.53}Ga_{0.47}As$ and $In_{0.52}Al_{0.48}As$ buffer layer lattice-matched to InP(001) substrate using molecular beam epitaxy. The effects of AlAs insertion on the InAs nanostructures were investigated and discussed.

Keywords nanostructures, MBE, InAs/InP(001)

PACS numbers 81.07.Ta, 81.16.Dn, 64.70.Nd

1 Introduction

Self-assembled InAs quantum dots (QDs) on both GaAs and InP substrates are promising for long wavelength optoelectronic device applications in the range 1.3–1.55 μm. The fabrication of InAs/GaAs QDs has achieved much progress in recent years. In comparison, the controlling of the emission wavelength from the InAs/InP QDs still remains a great challenge due to some complications and difficulties in the epitaxial growth of InAs/InP using molecular-beam epitaxy (MBE), metal-organic chemical vapor deposition (MOCVD), or chemical-beam epitaxy (CBE) [1,2]. The lattice mismatch between InAs and InP is 3.2 %, relatively small in comparison with 7 % in the InAs/GaAs system, and InGa(Al)As or InGaAsP alloy buffers may undergo spinodal decomposition [3, 4], resulting in the modification of the surface nano-morphology [5]. Due to these problems, the control is difficult for the InAs/InP nanostructures in both structure and composition, and the formation of InAs quantum dashes or wires instead of QDs was often observed on the InGaAs [5] or InAlAs buffer [6] which are weak in carrier confinement.

The formation of InAs QDs on InP substrate may be influenced by inserting a thin tensile-strained layer [7,8]. Moreover, in order to suppress the As/P exchange in CBE or MOCVD and to control both the size and composition of InAs QDs on the InP substrate, a method was recently proposed in which an ultrathin GaAs layer was inserted between the InAs QDs and the InGaAsP layer underneath [9,10]. Using this method, the emission wavelength from the MOCVD or CBE InAs QDs on InP(001) substrate can be tuned in the range from 1405 to 1750 nm. Furthermore, the insertion of an tensile-strained layer, AlAs or GaAs, beneath the InAs layer significantly alters the surface energy and the adatom diffusion on the growing surface [11], and remarkably modifies the formation of the InAs islands on InP(001). Therefore, the investigation on the effects of an AlAs layer on the formation of the InAs islands may help us gain some insight into the mechanism of the island formation via the Stranski-Krastanow mechanism.

In this work, the MBE InAs QDs were fabricated with inserting an AlAs layer of two or three monolayers (ML) beneath on the InP(001) substrate; the effects of the AlAs inserting were investigated, and the using of atomic force microscope (AFM) was discussed.

2 Experimental details

Seven samples, referred to as A–G, were grown on semi-insulating InP(001). All these epitaxial structures contain an InAs strained layer, four or six monolayers (ML) in common on the surface for the AFM observation. The $In_{0.53}Ga_{0.47}As$ alloy lattice-matched to InP substrate was used as a buffer for all the samples except sample G in which the $In_{0.52}Al_{0.48}As$ alloy was used. In samples C–G, an AlAs layer, 2- or 3-ML in thickness, is inserted beneath the InAs layer. The epitaxial structures together with the substrate tempera-

LÜ Xiao-jing, WU Ju (✉), XU Bo, ZENG Yi-ping, WANG Biao-qiang, WANG Zhan-guo
Institute of Semiconductors, Chinese Academy of Sciences, Beijing 100083, China
E-mail: wuju@red.semi.ac.cn

Received May 14, 2007

ture T_s for the deposition of InAs are summarized in Table 1.

Table 1 Epilayer structures and the substrate temperatures for the growth of InAs.

Sample	AlAs/ML	InAs/ML	Buffer	Temperature /°C
A	None	4	$In_{0.53}Ga_{0.47}As$	460
B	None	4	$In_{0.53}Ga_{0.47}As$	500
C	2	4	$In_{0.53}Ga_{0.47}As$	460
D	2	4	$In_{0.53}Ga_{0.47}As$	500
E	3	4	$In_{0.53}Ga_{0.47}As$	500
F	3	6	$In_{0.53}Ga_{0.47}As$	500
G	2	4	$In_{0.52}Al_{0.48}As$	500

For MBE growth, the InP substrate was deoxided at 540 °C, and the As_4 beam equivalent pressure (BEP) was kept at 4×10^{-6} Torr throughout the growth, except for migration enhanced the epitaxy (MEE) of AlAs [12]. After deoxidation, T_s was reduced to 510 °C for the growth of a 200-nm buffer layer, $In_{0.47}Ga_{0.53}As$ or $In_{0.52}Al_{0.48}As$, at the growth rate of 0.84 μm/h. Then, T_s was reduced to 460 °C or 500 °C for the deposition of the subsequent layers, AlAs and InAs. For the samples A and B, a 4-ML InAs layer was directly deposited on the surface of the InGaAs buffer layer at 460 °C and 500 °C, respectively. For samples C–G, an AlAs layer was deposited on the buffer, InGaAs or InAlAs, using the MEE method [12], and then a 4- or 6-ML InAs was deposited on AlAs at the rate of 0.1 ML/s. The MEE growth was carried out by alternatively depositing 1 ML Al and 3 s As, intervened by a 3 s all-stop in between, to obtain a relatively flat AlAs surface. After InAs deposition, T_s was immediately cooled down to 200 °C. The MBE growth is in situ monitored by using reflection of high energy electron diffraction (RHEED). Contact-mode AFM is used to characterize the QD surface morphology, and statistics is performed to obtain QD densities, sizes and size dispersions.

3 Results and discussion

3.1 Surface InAs morphology on InP(001) with an AlAs layer beneath

The InAs nano-morphology on InP(001) is far more complex than that on GaAs(001), and sensitive to many factors such as the AlAs inserting layer, substrate temperature, arsenic atmosphere [13], chemical composition of the buffer [5] and even the growth method of the buffer [14]. Figure 1

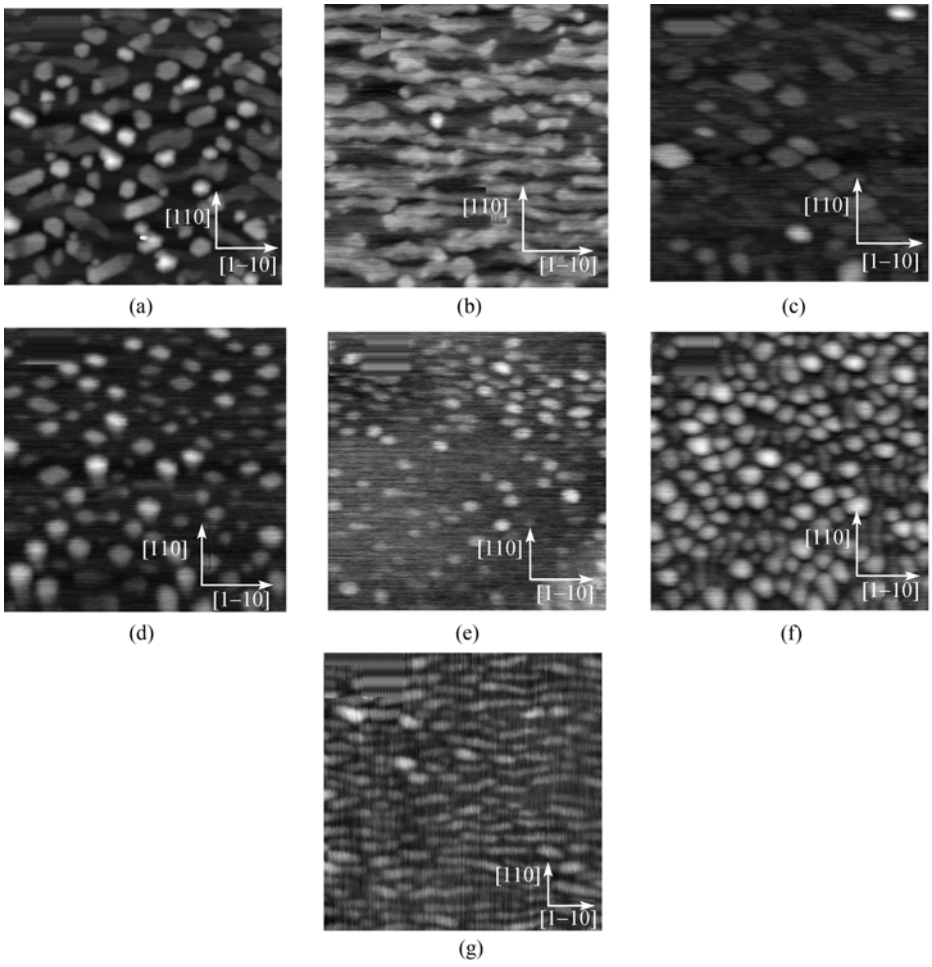

Fig. 1 AFM images of samples A–G in sequence, the scales of **(a)** and **(b)** are both 1×1 μm^2, and the scales of **(c)–(g)** are all 0.5×0.5 μm^2.

shows the AFM images of samples A–G, respectively. Without the AlAs layer beneath, as in samples A and B, the InAs nanostructures are irregular in shape, as shown in Fig. 1(a) and (b), which is similar to the observation on the InGaAs buffer as made by Li *et al*. [15]. However, as shown in Fig. 1(c)–(f), with inserting a 2-ML or 3-ML AlAs layer beneath, 3D InAs islands were formed on the InGaAs surface. The number density N, average island height H, average length L and width W along [1–10] and [110] directions on the substrate statistically obtained for the four samples are summarized in Table 2. However, on the InAlAs surface (sample G), the InAs wire-like structures were formed instead of islands.

Table 2 Island number density N (cm^{-2}), average height H (nm), average length L (nm) and average width W (nm), together with the relative fluctuations.

Sample	N /(10^{10} · cm^{-2})	H/nm ($\Delta H/H$)	L/nm ($\Delta L/L$)	W/nm ($\Delta W/W$)
C	1.8	2.8 (46 %)	40 (28 %)	16 (43 %)
D	4.6	3.3 (31 %)	33 (21 %)	13 (30 %)
E	2.6	2.3 (24 %)	35 (21 %)	14 (37 %)
F	7.1	3.6 (31 %)	33 (20 %)	16 (34 %)

The size dispersion of the InAs islands on InP(001) is very large in comparison to that in the MBE InAs/GaAs(001) system, in which the size dispersion, in general, is below 10 % [16]. Such a small size dispersion in the 3D InAs/GaAs(001) islands is generally attributed to the size-limiting effect produced by the lattice mismatch of ~7 % between InAs and GaAs [17,18]. However, the lattice mismatch in InAs/InP is only of ~3 %, much smaller than that in InAs/GaAs. Therefore, the size-limiting effect should be much less pronounced. As shown in Table 2, the maximum size dispersion of the InAs/InP islands reaches ~46 %, as in sample C.

Another prominent feature of the InAs/InP(001) islands with the AlAs inserting layer beneath is the relatively large anisotropy in shape. It can be calculated from the data in Table 2 that the ratio L/W is larger than 2 for all the samples. InAs wires or dashes are usually observed on the InP substrate with either InGaAs, InAlAs, or InP as a buffer due to some anisotropy in strain relaxation, atomic diffusion, or asymmetric spinodal decomposition. The insertion of an ultrathin AlAs layer beneath may reduce such anisotropies to some extent, and suppresses effectively the formation of InAs wires or dashes. However, the anisotropy of any kind may not be completely erased, and it would still be reflected by the anisotropic shape of the InAs islands with an AlAs layer beneath on the InGaAs buffer layer, as observed in this work.

3.2 Effects of the ultrathin AlAs layer on the surface energy

The lattice mismatch between AlAs and InP is ~3.7 %, and the ultrathin AlAs layer is tensile-strained on the surface of InGaAs or InAlAs lattice matched to InP(001). During the MBE growth of a 2- or 3-ML AlAs layer on the buffer, RHEED patterns along the [1–10] azimuth was streaky, which shows that the tensile-strained AlAs layer can be grown in two-dimension up to 3 ML. Figure 2(a) is the 5 × 5 μm^2 AFM image of sample F with a 3-ML AlAs layer beneath, and there are a large irregular pit with the number density of ~2 × 10^8 cm^2 on the surface. Figure 2(b) is a profile along the line across one of the pits as shown in Fig. 2(a). It shows the pit as deep as ~40 nm. Such deep pits are present in samples E and F, in which the AlAs layer is 3 ML in thickness. However, for samples C and D with the 2-ML AlAs layer, there are no such pits. It should be noted that these large pits are apparently different in size and depth from that as reported in Refs. [19, 20], the nucleation mechanism of which was attributed to the elastic strain. The formation of these large pits may be explained as follows. The tensile-strain in an ultrathin AlAs layer enhances significantly the surface energy. The larger the thickness of the AlAs layer, the more the surface energy is enhanced. For the 3-ML AlAs layer, the surface energy is enhanced so much that, at some sites, a large chemical-potential difference was produced between the AlAs surface and the regions beneath. Therefore, a large amount of matters are thermodynamically dug out of the buffer layer beneath. For the 2-ML AlAs, the

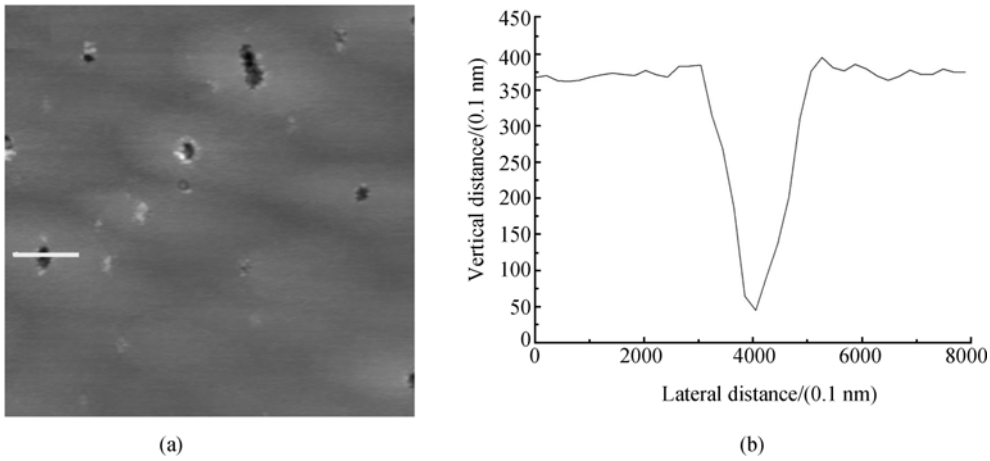

Fig. 2 **(a)** 5×5 μm^2 of sample F; **(b)** The profile of the pit along the line as marked on **(a)**.

surface energy is not enough for the large-pit formation.

The RHEED pattern demonstrated that the critical InAs deposition for the two- to three-dimensional transition is ~2.7 ML, slightly larger than 2.5 ML as usually reported on the InP(001) substrate. This shows that although the surface energy may be greatly enhanced, the critical thickness is not significantly altered in the InAs/InP system.

The growth conditions for samples D and E are the same except the AlAs thickness, which are 2- and 3-ML, respectively. Therefore, the surface energy of the latter should be larger than that of the former. Usually, for the self-assembling of InAs islands on a substrate [21], whether InP or GaAs, the less the surface energy, the easier the formation of the islands. Furthermore, the larger the surface energy, the larger the lateral size of the islands for the same parameters of growth and material. N is 4.6×10^{10} cm^2 in sample D, almost twice that of sample E. In addition, the lateral sizes of the islands in sample E are slightly larger than that of sample D. The distinction between the two samples in both N and lateral size is consistent with the general trend for the self-assembling of InAs islands on GaAs(001) or InP(001).

3.3 Effects of substrate temperature T_s

T_s has a significant impact on N, the island size [22] and the shape in InAs/GaAs(001) [23], and if T_s is raised by thirty or forty degrees, N may be reduced by an order of magnitude or even more. The effect of changing T_s on the InAs/GaAs nano-morphology is generally regarded as kinetic and attributed to the enhancement of the atomic diffusion at relatively high T_s. However, the case of InAs/InP is distinctively different. InAs was deposited at 460 °C in sample C with N~1.8×10^{10} cm^2, less than that for sample D by 40 °C with N~4.6×10^{10} cm^2. Strikingly, in contrast to InAs/GaAs, N is apparently reduced due to the decrease of T_s in InAs/InP. Furthermore, the InAs islands in sample C are larger in the average lateral size (40 nm in length, 16.4 nm in width), in contrast to the case of InAs/GaAs, while smaller in the average height (2.8 nm) than that of the sample D (33 nm in length, 13.3 nm in width and 3.3 nm in height). Figure 3 shows the histograms of height, length and width of samples C and D, respectively. Changing T_s has another obvious effect on the shape of the islands. As shown in Fig. 1(c), the InAs islands in sample C are nearly a parallelogram in shape, similar to that of MOCVD InAs islands grown on the InGaAs buffer on InP(001) [24], and significantly different from that in sample D with InAs deposited at 500 °C. In the latter, the shape of the islands is closer to an ellipse.

As described above, the effect of T_s on the density N in InAs/InP is opposite to InAs/GaAs, and this implies that T_s influences the atomic diffusion on the growing surface in a more complex manner. The thermodynamic equilibrium shape of self-assembled islands is currently unknown [25]. However, in the thermodynamic equilibrium, the shape of the InAs islands should mainly be determined by the lattice mismatch strain and the relevant material parameters, and the effect T_s should be less significant [22]. If the island shape is kinetically limited, T_s should have an important role in determining it. Lowering of T_s may significantly suppress the atomic diffusion and redistribution inside an InAs island on InP(001). The effect of T_s on the island shape, as observed on samples C and D, demonstrated that the island shape should be kinetically determined and far from thermodynamic equilibrium.

3.4 Effects of the InAs coverage

Both samples E and F were grown at 500 °C on the InGaAs buffer with 3-ML AlAs inserted beneath the InAs layer. In sample E, the InAs thickness is 4 ML, while in sample F it is

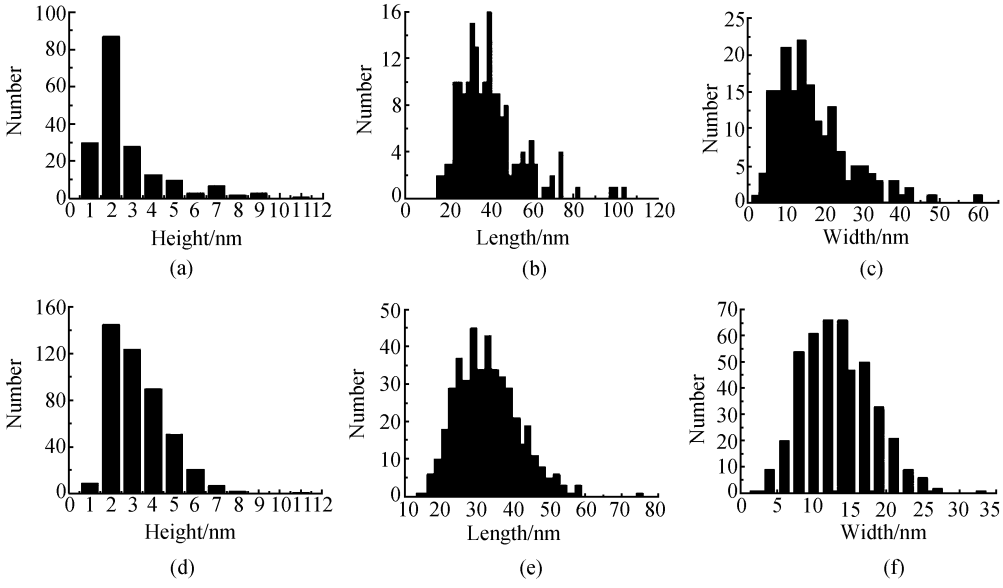

Fig. 3 Histograms of the size of InAs islands in samples C and D, **(a)** and **(d)** height, **(b)** and **(e)** length, **(c)** and **(f)** width.

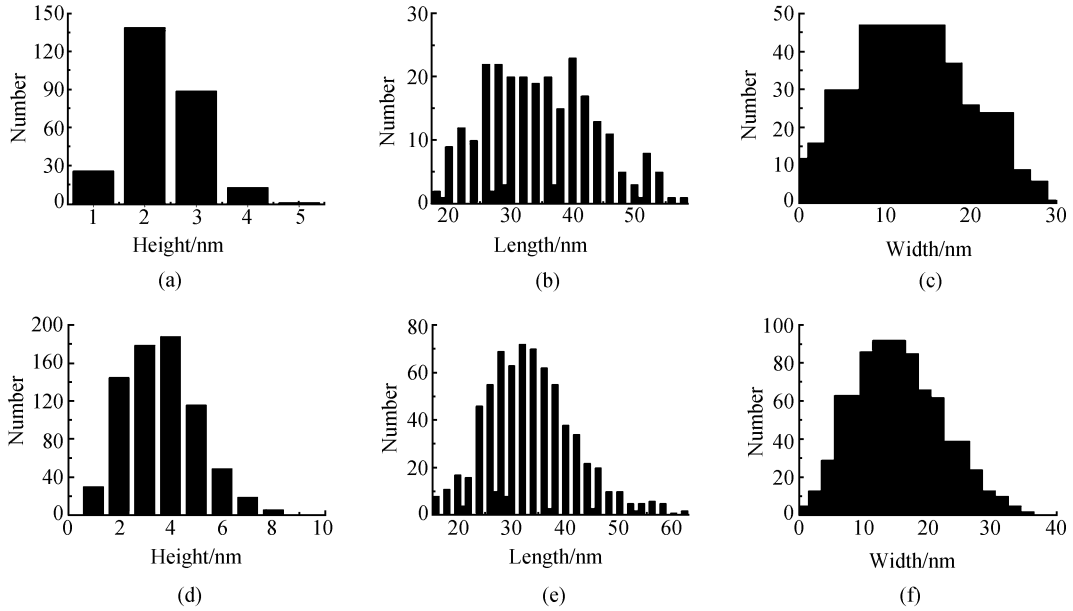

Fig. 4 Histograms of the size of InAs islands in samples E and F, **(a)** and **(d)** height, **(b)** and **(e)** length, **(c)** and **(f)** width.

6 ML. It can be seen from Table 2 that the 2-ML-InAs increment increases significantly N from 2.6×10^{10} cm^2 in sample E to 7.1×10^{10} cm^2 in sample F. In addition, the average island height was also increased by 1.3 nm with increasing InAs coverage, while the lateral dimensions is slightly different from one another.

Another effect of increasing InAs coverage is on the size distributions of the islands. Figure 4 shows the island distributions in height, length and width for samples E and F, respectively. In sample E with 4 ML InAs, the island height distribution is obviously biased weighted on the low-sized end, and the width distribution is scattered. In comparison, both the island height and width distributions of sample F with 6-ML InAs are closer to a Gaussian type.

It is well known that two- to three-dimension (2D-3D) transition is completed within ~0.2 ML InAs increment after the critical InAs deposition in MBE InAs/GaAs(001). After the 2D-3D transition, the island number density is nearly saturated, and the island size distribution is almost a Gaussian type with a nearly constant average size within a certain range of InAs increment [17]. The Gaussian distribution and a constant average size are characteristics for a matured InAs island ensemble before island coalescence occurs [26]. However, with the critical InAs deposition of ~2.7 ML for the 2D-3D transition in InAs/InP with an AlAs layer beneath, after more than 1.3 ML further InAs deposition beyond the critical InAs deposition, the InAs islands still evolves drastically until 6 ML InAs deposition. Therefore, the 2D-3D transitional process in the InAs/InP system should be elongated considerably in comparison with that in InAs/GaAs.

3.5 Effects of the buffer composition

The surface of nano-morphology is wire-like on the surface of sample G with the $In_{0.52}Al_{0.48}As$ buffer instead of $In_{0.53}Ga_{0.47}As$ as in other samples. This implies that inserting an AlAs layer beneath InAs almost has no effect in suppressing the formation of the InAs wires or dashes on the $In_{0.52}Al_{0.48}As$ buffer, in contrast to $In_{0.53}Ga_{0.47}As$.

A remarkable distinction between InAlAs and InGaAs is on the chemical instability of the alloys due to a positive enthalpy of mixing $\Delta H_m = x(1-x)\Omega$. The larger the interaction parameter Ω, the easier for the alloy decomposition to happen. The value of Ω for InAlAs is ~3 600 cal/mol, significantly lager than that of InGaAs (Ω ~2 490 cal/mol). Therefore, the $(InAs)_x(AlAs)_{1-x}$ nanostructure resulting from the spinodal decomposition in the InAlAs alloy is more significant than the corresponding $(InAs)_x(GaAs)_{1-x}$ one in the InGaAs alloy. The nanostructure in the InAlAs or InGaAs alloy is generally anisotropic along the [1–10] and [110] directions [27–29], and it may be the mechanism for the formation of InAs wires on the InP substrate [4]. It seems that such a mechanism can be effectively suppressed by the insertion of an ultrathin AlAs layer on the InGaAs buffer, while it still plays an important role in the self-assembling of InAs wires on the InAlAs buffer on the InP substrate.

4 Conclusion

The MBE InAs nanostructures on InP(001) with an ultrathin AlAs layer beneath were investigated using AFM. The effects on the InAs nanostructures of the ultrathin AlAs layer, substrate temperature, InAs coverage and buffer composition were revealed and discussed.

Acknowledgements This work was supported by the National Natural

Science Foundation of China (Grant Nos. 2006CB604904 and 60676029).

References

1. Notzel R. and Haverkort J. E. M., Adv. Funct. Mater., 2006, 16: 327
2. Barik S., Tan H. H., and Jagadish C., Nanotechnology, 2006, 17: 1867
3. LaPierre R. R., Okada T., Robinson B. J., Thompson D. A., and Weatherly G. C., J. Cryst. Growth, 1995, 155: 1
4. Grenet G., Gendry M., Oustric M., Robach Y., Porte L., Hollinger G., Marty O., Pitaval M., and Prierster C., Appl. Surf. Sci., 1998, 123/124: 324
5. Brault J., Gendry M., Grenet G., Hollinger G., Desieres Y., and Benyattou T., Appl. Phys. Lett., 1998, 73: 2932
6. Zhao F. A., Chen Y. H., Ye X. L., Jin P., Xu B., Wang Z. G., and Zhang C. L., J. Phys.: Condens. Matter, 2004, 16: 7603
7. Wang X. Q., Du G. T., Yin J. Z., Li M., Li M. T., Qu Y., Bo B. X., and Yang S. R., J. Cryst. Growth, 2002, 235: 60
8. Kim J. S., Lee J. H., Hong S. U., Han W. S., Kwack H. S., Lee C. W., and Oh D. K., J. Cryst. Growth, 2003, 259: 252
9. Gong Q., Notzel R., van Veldhoven P. J., Eijkemans T. J., and Wolter J. H., Appl. Phys. Lett., 2004, 84: 275
10. Anatathanasarn S., Notzel R., van Veldhoven P. J., van Otten F. W. M., Eijkemans T. J., and Wolter J. H., Appl. Phys. Lett., 2006, 88: 063105
11. Penev E., Kratzer P., and Scheffler M., Phys. Rev. B, 2001, 64: 085401
12. Horikoshi Y., Semicond. Sci. Technol., 1993: 1032
13. Brault J., Gendry M., Grenet G., Hollinger G., Olivares J., Salem B., Benyattou T., and Bremond G., J. Appl. Phys., 2002, 92: 506
14. Gonzalez L., Garcia J. M., Garcia R., Briones F., and Martinez-Pastor J., Appl. Phys. Lett., 2000, 76: 1104
15. Li H., Daniels-Race T., and Hasan M. A., Appl. Phys. Lett., 2002, 80: 1367
16. Moison J. M., Houzay F., Barthe F., and Leprince L., Appl. Phys. Lett., 1994, 64: 196
17. Kobayashi N. P., Ramachandran T. R., Chen P., and Madhukar A., Appl. Phys. Lett., 1996, 68: 3299
18. Barabasi A-L, Appl. Phys. Lett., 1997, 70: 2565
19. Chokshi N. S. and Millunchick J. M., Appl. Phys. Lett., 2000, 76: 2382
20. Chokshi N., Bouviller M., and Millunchick J. M., J. Cryst. Growth, 2000, 236: 563
21. Shchukin V. A., Ledentsov N. N., Kopev P. S., and Bimberg D., Phys. Rev. Lett., 1995, 75: 2968
22. Solomon G. S., Trezza J. A., and Harris J. S., Appl. Phys. Lett., 1995, 66: 991
23. Saito H., Nishi K., and Sugou S., Appl. Phys. Lett., 1999, 74: 1224
24. Hwang H. D., Yoon S., Kwon H., Yoon E., Kim H. S., Lee J. Y., and Cho B., Appl. Phys. Lett., 2004, 85: 6383
25. Kratzer P., Liu Q. K. K., Acosta-Diaz P., Manzano C., Costantini G., Songmuang R., Rastelli A., Schmidt O. G., and Kern K., Phys. Rev. B, 2006, 73: 205347
26. Schmidt K. H., Medeiros-Ribeiro G., Kunze U., Abstreiter G., Hagn M., and Petroff P. M., J. Appl. Phys., 1998, 84: 4268
27. Chou S. T., Cheng K. Y., Chou L. J., and Hsieh K. C., Appl. Phys. Lett., 1995, 66: 2220
28. Mirecky J. M., Twesten R. D., Follstaedt D. M., Lee S. R., Jones E. D., Zhang Y., Ahrenkiel S. P., and Mascrenhas A., Appl. Phys. Lett., 1997, 70: 1402
29. Francoeur S., Norman A. G., Hanna M. C., Mascarenhas A., Reno J. L., Follstaedt D. M., and Lee S. R., Mater. Sci. and Eng. B, 2002, 88: 118